Physics-Aware Sparse Signal Recovery Through PDE-Governed Measurement Systems

Tadashi Wadayama
Nagoya Institute of Technology
wadayama@nitech.ac.jp

Koji Igarashi
Osaka University
iga.koji.es@osaka-u.ac.jp

Takumi Takahashi
Osaka University
takahashi@comm.eng.osaka-u.ac.jp

Abstract—This paper introduces a novel framework for physics-aware sparse signal recovery in measurement systems governed by partial differential equations (PDEs). Unlike conventional compressed sensing approaches that treat measurement systems as simple linear systems, our method explicitly incorporates the underlying physics through numerical PDE solvers and automatic differentiation (AD). We present physics-aware iterative shrinkage-thresholding algorithm (PA-ISTA), which combines the computational efficiency of ISTA with accurate physical modeling to achieve improved signal reconstruction. Using optical fiber channels as a concrete example, we demonstrate how the nonlinear Schrödinger equation (NLSE) can be integrated into the recovery process. Our approach leverages deep unfolding techniques for parameter optimization. Numerical experiments show that PA-ISTA significantly outperforms conventional recovery methods. While demonstrated on optical fiber systems, our framework provides a general methodology for physics-aware signal recovery that can be adapted to various PDE-governed measurement systems.

I. INTRODUCTION

Over the past two decades, compressed sensing [1], [2] has revolutionized signal processing by enabling efficient reconstruction of signals from far fewer measurements than traditional sampling methods would require. This breakthrough has been particularly impactful in scenarios where signals exhibit sparsity, i.e., a property where the signal can be represented by only a few non-zero coefficients in an appropriate basis.

The development of efficient sparse signal recovery algorithms [3] has been crucial to the practical success of compressed sensing. These algorithms typically solve an optimization problem that balances measurement fidelity with sparsity-promoting regularization. Notable examples include basis pursuit, least absolute shrinkage and selection operator (LASSO) [4], [5], and various iterative methods such as iterative shrinkage-thresholding algorithm (ISTA) [6], [7]. These approaches have found applications in diverse fields, from medical imaging to astronomical observation.

However, many real-world inverse problems involve physical processes that cannot be adequately modeled by simple linear measurements. Examples include nonlinear optical effects like the Kerr effect in fiber optics, wave propagation in nonlinear acoustic media, and electromagnetic interactions with nonlinear meta-materials. In such cases, the reconstruction problem becomes significantly more challenging as it must account for the underlying physics governing signal propagation and measurement.

There is growing recognition that incorporating explicit physical models into the inverse problem framework could potentially improve quality of solutions. A prominent example is physics informed neural networks (PINNs) [8]. Beyond solving forward problems, PINNs have proven particularly effective for partial differential equation (PDE)-based inverse problems, highlighting the significant potential of integrating physical models with machine learning methodologies. This PINN approach represents a promising direction for applications where physical effects significantly influence the measurement process, although its full potential and limitations remain largely unexplored.

Recent advances in computational techniques, particularly automatic differentiation (AD) [10], have opened new possibilities for incorporating physical models into signal processing frameworks. In this paper, we propose a general framework for physics-aware sparse signal recovery that incorporates PDEs describing the underlying physical phenomena. While our methodology is applicable to a wide range of physical systems governed by PDEs, we demonstrate its effectiveness using optical fiber channels [9] as a concrete and challenging example. The key innovation lies in our use of AD mechanism to compute gradients through a numerical PDE solver, enabling efficient optimization despite the complexity of the physical system. The proposed framework is general enough to be adapted to other physical systems where the underlying physics can be described by PDEs, such as heat conduction processes, wave propagation in elastic media, or fluid dynamics.

II. PRELIMINARIES

A. Sparse signal recovery problem

In this subsection, we review the fundamentals of compressed sensing with simple linear measurements. Let us consider a sparse signal $s \in \mathbb{R}^n$, where sparsity implies that only a small fraction of its elements are non-zero relative to the dimension n. The measurement process can be described by a linear model:

$$y = As + w, \tag{1}$$

where $y \in \mathbb{R}^m$ $(m < n)$ represents the measurement vector, $A \in \mathbb{R}^{m \times n}$ is the measurement matrix, and $w \in \mathbb{R}^m$ denotes the measurement noise. In the sparse signal recovery problem, the objective is to recover the original signal s from the given

measurement vector $\boldsymbol{y}$ with maximum possible accuracy. The observer has access only to $\boldsymbol{y}$ and $\boldsymbol{A}$. It is important to note that since $m < n$, without considering the sparsity of the original signal $\boldsymbol{s}$, this becomes an underdetermined problem with no unique solution.

A widely adopted approach to sparse signal reconstruction is the Lasso [4], [5], which formulates the problem as a regularized least squares optimization. The Lasso framework reconstructs the sparse signal by solving the convex optimization problem:

$$\hat{\boldsymbol{s}} \equiv \text{argmin}_{\boldsymbol{x} \in \mathbb{R}^n} \left(\frac{1}{2} \|\boldsymbol{y} - \boldsymbol{A}\boldsymbol{x}\|_2^2 + \lambda \|\boldsymbol{x}\|_1 \right), \quad (2)$$

where $\hat{\boldsymbol{s}}$ represents the reconstructed signal and $\lambda (> 0)$ is a regularization parameter. The objective function consists of two terms: a quadratic data fidelity term that measures the reconstruction error, and an L1-norm regularization term that promotes sparsity in the solution. The parameter λ controls the trade-off between these competing objectives.

B. ISTA *for sparse signal recovery*

ISTA [6], [7] is a well-known proximal gradient method for solving the Lasso problem. In this section, we aim to derive the ISTA update equations. For the Lasso minimization problem, let us define $f(\boldsymbol{x}) \equiv \frac{1}{2} \|\boldsymbol{y} - \boldsymbol{A}\boldsymbol{x}\|_2^2$, and $h(\boldsymbol{x}) \equiv \lambda \|\boldsymbol{x}\|_1$. It is important to note that since the L1 regularization term is non-differentiable, algorithms that assume differentiability of the objective function cannot be applied. The gradient vector of the squared error term $f(\boldsymbol{x})$ is given by

$$\nabla f(\boldsymbol{x}) = \boldsymbol{A}^T (\boldsymbol{A}\boldsymbol{x} - \boldsymbol{y}). \quad (3)$$

The proximal operator [12] of the L1 regularization term $\tau \|\boldsymbol{x}\|_1$,

$$\text{prox}_{\tau\|\boldsymbol{x}\|_1}(\boldsymbol{x}) = S_\tau(\boldsymbol{x}) \equiv \text{sign}(x) \max\{|x| - \tau, 0\}, \quad (4)$$

is the soft-thresholding function. In sparse signal reconstruction problems, the proximal operator corresponding to the regularization term is sometimes called the *shrinkage function*.

ISTA is a proximal gradient method [12] derived from the Lasso problem and is defined by the iterative equations:

$$\boldsymbol{z}^{(k)} = \boldsymbol{x}^{(k)} - \eta \boldsymbol{A}^T (\boldsymbol{A}\boldsymbol{x}^{(k)} - \boldsymbol{y}) \quad (5)$$

$$\boldsymbol{x}^{(k+1)} = S_{\eta\lambda}(\boldsymbol{z}^{(k)}), \quad k = 0, 1, \dots \quad (6)$$

Eq.(5) is called the *gradient descent step*, and Eq.(6) is called the *shrinkage step*. Here, the step size parameter η is a real constant, and ISTA converges to the Lasso solution when $\eta < 1/\Gamma$ where Γ is the maximum eigenvalue of the Gram matrix $\boldsymbol{A}^T \boldsymbol{A}$.

C. *Nonlinear Schrödinger Equation (NLSE)*

We consider the NLSE:

$$\frac{\partial U}{\partial z} = -\frac{i\beta_2}{2} \frac{\partial^2 U}{\partial t^2} + i\gamma |U|^2 U, \quad (7)$$

where i denotes the imaginary unit [9]. The variables z and t represent the position in a fiber and time, respectively. The

function $U(t, z)$ describes the optical field in the optical fiber. The NLSE plays a fundamental role in single-mode optical fiber communications, where it governs signal propagation by describing the evolution of optical pulse shapes and phases along the fiber length. This evolution is influenced by physical effects such as dispersion and nonlinearity. The parameter $\beta_2 \in \mathbb{R}$ is the dispersion constant and the nonlinear coefficient $\gamma \in \mathbb{R}$ characterizes the strength of the fiber nonlinearity.

D. *State Split Fourier Method (SSFM)*

The nonlinear Schrödinger equation involves both linear dispersion terms and nonlinear effects, making it challenging to solve directly. The split-step Fourier method (SSFM) [9] provides an efficient numerical approach by leveraging the distinct characteristics of these terms. Consider the nonlinear Schrödinger equation: $\partial A / \partial z = (\hat{D} + \hat{N})A$, where A is the complex envelope of the optical field, $\hat{D}$ represents the linear dispersion operator in the frequency domain, and $\hat{N}$ represents the nonlinear operator in the time domain.

The fundamental principle of SSFM lies in its approach to handling operators that cannot be solved simultaneously. While the combined effect of dispersion and nonlinearity cannot be computed exactly, SSFM provides an efficient approximation by treating these effects separately over small propagation steps Δz. The method iterates the following stages at each step:

1) The signal is transformed to the frequency domain using Fast Fourier Transform (FFT);
2) The dispersion effect is applied in the frequency domain using the operator $\hat{D}$;
3) The signal is then transformed back to the time domain through inverse FFT;
4) The nonlinear effects are computed in the time domain using the operator $\hat{N}$;

This approach is particularly efficient because the dispersion operator $\hat{D}$ takes a simple multiplicative form in the frequency domain, while the nonlinear operator $\hat{N}$ is easily computed in the time domain. The FFT provides an efficient means to switch between these domains, making the overall method computationally practical.

III. SPARSE SIGNAL RECOVERY PROBLEM

A. *Overview*

Although our physics-aware sparse signal recovery framework is applicable to a wide range of partial differential equations, we demonstrate its effectiveness using the NLSE (7) as a concrete example. In our problem formulation, we consider a system where a sensing device at the fiber input ($z = 0$) injects a waveform $U(t, 0)$ consisting of several sparse pulses, which can be considered as the *target sparse signals*. As this signal propagates through the fiber, it is observed by a detector placed at the fiber output ($z = L$). Our goal is to reconstruct the target sparse signal from these output measurements, effectively recovering the input signal through the nonlinear fiber channel. As the optical signal propagates through the fiber, the waveform evolves according to the NLSE
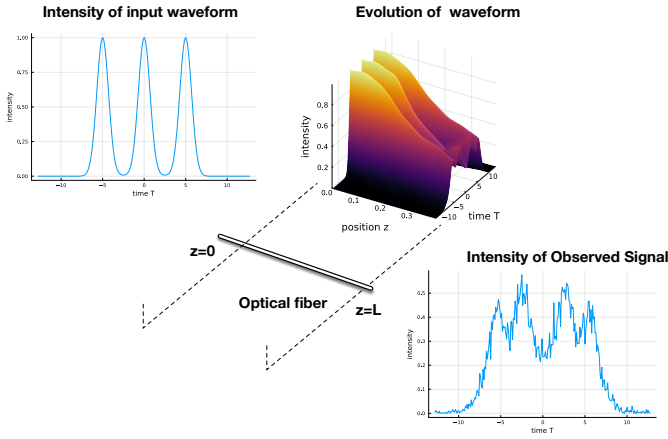
Fig. 1. Visualization of signal propagation through an optical fiber. The left panel displays the intensity profile of the input signal $|U(t,0)|^2$ at the fiber input. The center panel shows a three-dimensional visualization of the signal intensity $|U(t,z)|^2$, illustrating how the waveform evolves as it propagates along the fiber length z. The right panel presents the measured intensity profile $|U(t,L)|^2$ at the fiber output, including the effects of measurement noise.

(7) with increasing z. The signal recovery problem can be stated as follows: given a noisy observation of the waveform $U(t,L)$ at position $z = L$, estimate the original sparse signal $U(t,0)$. In other words, we aim to detect the set of sparse pulses at the fiber input ($z = 0$) using measurements obtained at the fiber output ($z = L$).

B. Details

Let us define a Gaussian-shaped pulse function as

$$\phi(x) \equiv \exp\left(-x^2/(2T_0^2)\right), \qquad (8)$$

where T_0 represents the pulse half-width (measured at the $1/e$-intensity point). We model the initial waveform as a linear combination of Gaussian-shaped pulses $\phi(x - p_i)$ centered at positions $p_i(i \in [n])$. Specifically, the input waveform at the fiber input ($z = 0$) is given by

$$U(\tau, 0) = \sum_{i=1}^{n} s_i \phi(\tau - p_i), \qquad (9)$$

where $\boldsymbol{s} \equiv (s_1, s_2, \ldots, s_n) \in \mathbb{C}^n$ represents a sparse complex vector with only k non-zero components ($k \ll n$). This input waveform serves as the boundary condition for the NLSE (7). Let $U(t, z; \boldsymbol{s})$ denote the unique solution of the NLSE (7) that satisfies this boundary condition. At the fiber output, the detector performs measurements by sampling the waveform at specific time points $q_i(i \in [m])$, yielding the sampled values:

$$y_i = U(q_i, L; \boldsymbol{s}) + n_i, \quad i \in [m], \qquad (10)$$

where each noise term n_i follows a complex Gaussian distribution, i.e., $n_i \sim \mathcal{CN}(\boldsymbol{0}, \sigma^2)$. Figure 1 visualizes behavior of signal propagation through an optical fiber.

Based on the above formulation, we can now precisely define our sparse signal recovery problem. Given the observation vector $\boldsymbol{y} \equiv (y_1, y_2, \ldots, y_m) \in \mathbb{C}^m$ at the fiber output,

our objective is to accurately reconstruct the original sparse complex vector $\boldsymbol{s}$. This recovery problem presents significant challenges due to the nonlinear nature of the wave evolution governed by the NLSE, making it fundamentally different from conventional sparse recovery problems.

IV. PROPOSED METHOD

A. Lasso-like formulation

To address the sparse signal recovery problem described above, it is natural to consider an optimization-based approach analogous to the classical Lasso formulation. We propose to minimize a Lasso-like objective function $F : \mathbb{C}^n \to \mathbb{R}$ defined as

$$F(\boldsymbol{s}) \equiv \|\boldsymbol{y} - f(\boldsymbol{s})\|_2^2 + \lambda \|\boldsymbol{s}\|_1, \qquad (11)$$

where $f(\boldsymbol{s}) \equiv (U(q_1, L; \boldsymbol{s}), \ldots, U(q_m, L; \boldsymbol{s}))$ represents the noiseless output of the nonlinear fiber channel at the sampling points. The first term measures the fidelity between the observed samples and the predicted output, while the second term promotes sparsity in the solution. By minimizing this objective function, we aim to obtain a sparse solution that is consistent with both the observed data and the underlying physics described by the NLSE.

B. Physics-aware ISTA

The optimization problem formulated in the previous subsection can be expressed as

$$\text{minimize}_{\boldsymbol{s} \in \mathbb{C}^n} F(\boldsymbol{s}), \qquad (12)$$

where the objective function becomes non-convex when the fiber channel exhibits significant nonlinearity. Despite this non-convexity, we propose to adapt the ISTA framework to minimize $F(\boldsymbol{s})$. This leads to a complex-valued variant of the ISTA algorithm:

$$\boldsymbol{z}^{(k)} = \boldsymbol{x}^{(k)} - \eta^{(k)} \nabla_{\boldsymbol{x}^{(k)}} \|\boldsymbol{y} - f(\boldsymbol{x}^{(k)})\|_2^2 \qquad (13)$$

$$\boldsymbol{x}^{(k+1)} = T_{\theta^{(k)}}(\boldsymbol{z}^{(k)}), \quad k = 0, 1, \ldots, \qquad (14)$$

where $T_\tau : \mathbb{C} \to \mathbb{C}$ denotes the complex shrinkage operator defined by

$$T_\tau(x) \equiv (x/|x|)\{\max |x| - \tau, 0\}. \qquad (15)$$

It is important to note that the objective function F defined over the complex field $\mathbb{C}$ is non-holomorphic. Consequently, when computing the gradient $\nabla_{\boldsymbol{x}^{(k)}} \|\boldsymbol{y} - f(\boldsymbol{x}^{(k)})\|_2^2$, we must employ the *Wirtinger derivative*, which provides the appropriate framework for differentiation of non-holomorphic functions. Wirtinger calculus provides a rigorous framework for optimization in the complex domain. This approach treats a complex variable z and its conjugate z^* as independent variables, defining the derivatives:

$$\frac{\partial g}{\partial z} = \frac{1}{2}\left(\frac{\partial g}{\partial x} - i\frac{\partial g}{\partial y}\right), \quad \frac{\partial g}{\partial z^*} = \frac{1}{2}\left(\frac{\partial g}{\partial x} + i\frac{\partial g}{\partial y}\right) \qquad (16)$$

for a real-valued function $g(z)$ where $z = x + iy$. These Wirtinger derivatives enable gradient-based optimization of

our non-holomorphic objective function in the complex domain. Namely, the conjugate derivative can be used in gradient descent processes. In our implementation, AD naturally computes these Wirtinger derivatives when operating on complex variables.

A significant implementation challenge lies in computing the gradient term in (13), since the NLSE (7) rarely admits closed-form solutions. To address this challenge, we employ a numerical PDE solver, i.e., the SSFM solver, to approximate the channel output f. The approximate noiseless output at the sampling points is defined as

$$\hat{f}(\boldsymbol{s}) \equiv (\hat{U}(q_1, L; \boldsymbol{s}), \ldots, \hat{U}(q_m, L; \boldsymbol{s})), \tag{17}$$

where $\hat{U}(\cdot, \cdot; \boldsymbol{s})$ represents the approximate solution obtained through the SSFM solver. By leveraging AD, we can efficiently compute the Wirtinger gradient $\nabla_{\boldsymbol{x}^{(k)}} \|\boldsymbol{y} - \hat{f}(\boldsymbol{x}^{(k)})\|_2^2$. This leads to a recursive formula of *physics-aware ISTA (PA-ISTA) algorithm*:

$$\boldsymbol{z}^{(k)} = \boldsymbol{x}^{(k)} - \eta^{(k)} \nabla_{\boldsymbol{x}^{(k)}} \|\boldsymbol{y} - \hat{f}(\boldsymbol{x}^{(k)})\|_2^2 \tag{18}$$

$$\boldsymbol{x}^{(k+1)} = T_{\theta^{(k)}}(\boldsymbol{z}^{(k)}), \quad k = 0, 1, \ldots. \tag{19}$$

The complete description of physics-aware sparse signal recovery algorithm is given in Algorithm 1. The choice of the squared error function as a loss function is motivated by our assumption of additive white Gaussian noise in the system model. For non-Gaussian noise scenarios, the error function can be appropriately modified to match the underlying noise statistics.

We initialize the state vector using the zero-forcing solution obtained through the *Backpropagation method (BP)* [1] [13], a widely established technique for nonlinearity compensation in optical fiber communications. BP reconstructs the input signal by numerically solving the NLSE in reverse, with the signs of both dispersion and nonlinearity coefficients inverted. This approach effectively "undoing" the channel effects by propagating the received signal backwards through a *virtual fiber with inverse channel parameters*.

In the ideal case of noiseless transmission, BP can achieve perfect signal recovery. However, in practical scenarios where noise is present, BP's performance degrades significantly due to its inherent noise amplification characteristics.

The proposed algorithm exhibits a double-loop structure: an outer loop implementing the proximal gradient iterations, and an inner loop executing the SSFM. The computational complexity of the SSFM solver scales with the number of grid points, requiring $O(N_t N_z)$ operations, where N_t and N_z represent the number of grids in t and z direction, respectively. When $\max\{n, m\} < \min\{N_z, N_t\}$, the overall computational complexity of the algorithm becomes $O(U N_t N_z)$. A practical trade-off exists between computational efficiency and solution accuracy. While using a coarser grid (smaller N_t and N_z) reduces computational time, it may compromise the quality of the recovered signal. Therefore, careful selection of grid

[1]Note that this backpropgation method is not for computing the gradients.

parameters is crucial for balancing computational complexity against recovery performance.

Algorithm 1 Physics-Aware ISTA (PA-ISTA)

1: Set the initial state $\boldsymbol{x}^{(0)} := BP(\boldsymbol{y})$.
2: **for** $k := 0$ to $U - 1$ **do**
3:     Let $b(t) := \sum_{i=1}^{n} x_i^{(k)} \phi(t - p_i)$.
4:     Solve the NLSE (7) with the boundary condition $\hat{U}(t, 0; \boldsymbol{x}^{(k)}) = b(t)$ by using the SSFM solver.
5:     Generate reconstructed samples:

$$r_i := \hat{U}(q_i, L; \boldsymbol{x}^{(k)}), \ i \in [m].$$

6:     Let $r(\boldsymbol{x}^{(k)}) \equiv (r_1, r_2, \ldots, r_m)$.
7:     Compute the Wirtinger gradient by AD:

$$\boldsymbol{g} := \nabla_{\boldsymbol{x}^{(k)}} \|\boldsymbol{y} - \boldsymbol{r}(\boldsymbol{x}^{(k)})\|_2^2.$$

8:     Execute the GD process: $\boldsymbol{z}^{(k)} := \boldsymbol{x}^{(k)} - \eta^{(k)} \boldsymbol{g}$.
9:     Execute the shrinkage process: $\boldsymbol{x}^{(k+1)} := T_{\theta^{(k)}}(\boldsymbol{z}^{(k)})$.
10: **end for**
11: Output $\hat{\boldsymbol{s}} \equiv \boldsymbol{x}^{(U)}$ as the estimate.

C. Deep Unfolding (DU) for Parameter Tuning

The performance of PA-ISTA critically depends on the choice of two key parameters: the step size parameter $\eta^{(k)}$ and the shrinkage parameter $\theta^{(k)}$. These parameters significantly influence both the convergence behavior and the quality of the estimated signal. Unlike conventional ISTA for linear measurements, where theoretical guidelines exist for parameter selection (e.g., $\eta < 1/\Gamma$), the nonlinear nature of our physics-aware framework makes it challenging to establish general rules for parameter setting. To address this challenge, we propose to leverage *deep unfolding (DU)* [14]–[16], a technique that bridges iterative optimization algorithms and deep learning. Deep unfolding treats each iteration of an optimization algorithm as a layer in a neural network, allowing the algorithm's parameters to be learned from training data. In this approach, the iterations of PA-ISTA are "unfolded" into a fixed-depth network structure, where each layer maintains the same form as a PA-ISTA iteration but with learnable parameters. This transformation enables us to optimize the step size and shrinkage parameters through standard neural network training procedures while preserving the physics-aware nature of the algorithm.

Applying deep unfolding to PA-ISTA presents a unique technical challenge due to the *nested structure of gradient computations*. In each iteration of PA-ISTA, AD is used to compute gradients through the physics model with the SSFM solver. When we attempt to unfold PA-ISTA into a neural network structure, we encounter a situation where AD needs to be performed at two different levels: one for the physics model within each iteration, and another for the end-to-end training of the unfolded network. This nested AD structure

poses a significant implementation challenge because most of AD do not support nested AD computations. i.e., typical AD engines are designed to handle a single level of gradient computation. This limitation creates a fundamental obstacle for parameter tuning through DU, as we cannot directly apply standard neural network training procedures to our unfolded PA-ISTA architecture. Resolving this nested AD challenge is crucial for successfully implementing the deep unfolding approach for PA-ISTA parameter optimization.

To overcome this implementation challenge, we propose the *store-and-replay method*, which effectively decouples the two levels of AD by executing PA-ISTA iterations twice in a specific manner. The key idea is to separate the physics-based Wirtinger gradient computation from the DU-parameter optimization process. Algorithm 2 presents a pseudo code of the store-and-replay method. In the first pass (Store phase), we execute PA-ISTA iterations with AD enabled for the Wirtinger derivative. The second pass (Replay phase) then replicates the same PA-ISTA iterations but with a crucial difference; the gradients are retrieved from the storage. This two-pass approach successfully avoids nested AD while maintaining the mathematical equivalence to the original algorithm. The store-and-replay method enables us to apply DU for parameter tuning by effectively separating the physics-based gradient computation from the DU parameter optimization process.

Algorithm 2 Pseudo code of store-and-replay method

1: Iterate the following two phases with a distinct pair $(\boldsymbol{y}, \boldsymbol{s})$.

2: **[Store phase]** Compute Wirtinger gradients through the SSFM by AD.
3: Store these gradient vectors in a storage.
4: Execute standard PA-ISTA updates (without DU-training).

5: **[Replay phase]** Retrieve the pre-computed gradient vectors from the storage. Note that the initial state vector must be exactly the same as that used in the store phase.
6: Use these stored gradients for the PA-ISTA updates.
7: Enable DU parameter learning during replay phase.

D. Estimation of NLSE Parameters

Our discussion of PA-ISTA has thus far assumed perfect knowledge of the NLSE parameters, specifically the dispersion coefficient β_2 and the nonlinearity coefficient γ. In practical scenarios, however, these parameters are often unknown and must be estimated from measurements. This parameter uncertainty presents an additional challenge for physics-aware signal recovery, as incorrect parameter values can significantly degrade the recovery performance of PA-ISTA.

When the assumed parameters in the SSFM solver deviate from their true values, the numerical solution of the NLSE no longer accurately represents the actual signal propagation, leading to incorrect gradient computations and subsequently poor recovery performance. This sensitivity highlights the

importance of accurate parameter estimation for successful implementation of physics-aware recovery methods.

In oder to achieve accurate parameter estimation, we propose a parameter estimation method based on solving the following least square problem:

$$\text{minimize } _{\beta_2 \in \mathbb{R}, \gamma \in \mathbb{R}} \|\boldsymbol{y} - \boldsymbol{r}(\boldsymbol{s})\|_2^2, \quad (20)$$

where $\boldsymbol{s}$ represents a *known sparse pilot signal*, and $\boldsymbol{y}$ is the corresponding noisy observation vector obtained at the detector. This formulation seeks to find the NLSE parameters that best explain the observed signal propagation for the known pilot signal. The optimization problem can be solved using gradient descent, where the gradients with respect to β_2 and γ are efficiently computed through AD. This approach leverages the same computational framework used in PA-ISTA, making it naturally compatible with our physics-aware recovery scheme.

However, it is important to note that this minimization problem is inherently non-convex, introducing the possibility of the gradient descent process converging to undesirable stationary points. Consequently, the quality of the parameter estimates can be highly dependent on the initial values chosen for the optimization process. This sensitivity to initialization suggests the need for careful selection of starting points, possibly incorporating prior knowledge about typical parameter ranges in optical fiber systems.

V. NUMERICAL EXPERIMENTS

A. Signal Recovery Performance of PA-ISTA

We conducted extensive numerical experiments to evaluate the signal recovery performance of PA-ISTA. The simulations were performed using the following parameter setting. For the NLSE parameters, we set the dispersion constant β_2 to 10 and the nonlinear coefficient γ to 2. The pulse half-width T_0 was set to 1, resulting in a dispersion length $L_D \equiv T_0^2/|\beta_2| = 0.1$, and nonlinear length $L_{NL} \equiv 1/\gamma = 0.5$. These parameters were chosen to represent typical propagation conditions where both dispersion and nonlinear effects significantly influence the signal evolution. The SSFM solver was configured with a spatial step size (z-direction) of $l = 0.01$ and a temporal step size (t-direction) of $h = 0.3$. The temporal grid consisted of $m = 256$ points spanning the interval $[-38.4, 38.4]$, providing sufficient resolution for accurate waveform propagation simulation. For our experiments, we generated sparse test vectors with the following parameters. Each test vector had length $n = 30$ with exactly $k = 3$ non-zero elements, representing a sparse signal. The positions of the non-zero elements were randomly distributed across the vector following a uniform distribution. The values of the non-zero elements were complex numbers, each with unit magnitude ($|s_i| = 1$) but with uniformly randomly chosen phases.

The signal propagation and measurement were simulated over a distance of $L = 5L_D = 0.5$, requiring 50 iterations of the SSFM solver. To generate received signals, we synthesized the received waveform using the SSFM solver with the previously specified parameters. This approach allows us to evaluate

the recovery performance under well-controlled conditions while maintaining the essential nonlinear characteristics of optical fiber propagation. We used $q_i = -38.4 + ih(i = 0, 1, \ldots, 511)$ as sensing positions. The simulation code is implemented using Julia 1.9 and AD mechanism in Zygote.jl.

The deep unfolding training was conducted under the following experimental conditions. We set the signal-to-noise ratio to $SNR \equiv 1/\sigma^2 = 5$ dB. The network was trained for 100 iterations, with PA-ISTA configured to perform 30 iterations per forward pass. The step size parameters $\eta^{(k)}$ were initialized to 0.01, and the shrinkage parameters $\theta^{(k)}$ were initialized to 0.001 for $k = 0, 1, \ldots, 29$. These initial parameters were found by an ad hoc manner. For optimization of the learnable parameters, we employed the Adam optimizer [18] with a learning rate of 10^{-4} to simultaneously update both $\eta^{(k)}$ and $\theta^{(k)}$. The deep unfolding architecture was implemented following the methodology described in [17].

Figure 2 presents an example of sparse signal recovery using PA-ISTA with parameters optimized through deep unfolding. Panel (c) shows the recovered signal, which closely matches the original input waveform shown in panel (a), demonstrating the effectiveness of our approach. For comparison, panel (d) shows the result of conventional backpropagation-based recovery $BP(\boldsymbol{y})$. The comparison clearly illustrates that backpropagation fails to provide robust recovery in the presence of observation noise, whereas PA-ISTA maintains reliable performance under these challenging conditions.
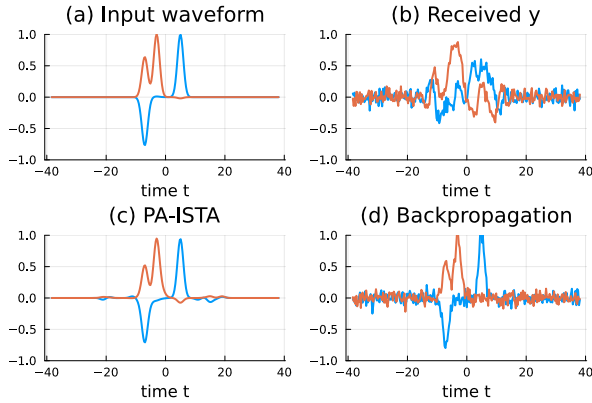

Fig. 2. Example of signal recovery. PA-ISTA with DU-optimized parameters were used (Blue:real part, Red: imaginary part). The SNR was set to 5 dB.

Figure 3 illustrates the values of the optimized parameters $\eta^{(k)}$ and $\theta^{(k)}$, alongside their initial values before training. A notable observation is the time-varying behavior of the optimized step size $\eta^{(k)}$, which suggests that different step sizes are beneficial at different stages of the recovery process. This adaptive nature of the parameters, discovered through DU, contrasts with conventional approaches that typically employ fixed parameters throughout the iterations.

Figure 4 compares the mean squared error (MSE) performance of PA-ISTA under different SNR conditions (5dB). The MSE is defined as $\mathsf{E}\left[\|\boldsymbol{s} - \hat{\boldsymbol{s}}\|_2^2\right]$, where $\boldsymbol{s}$ represents
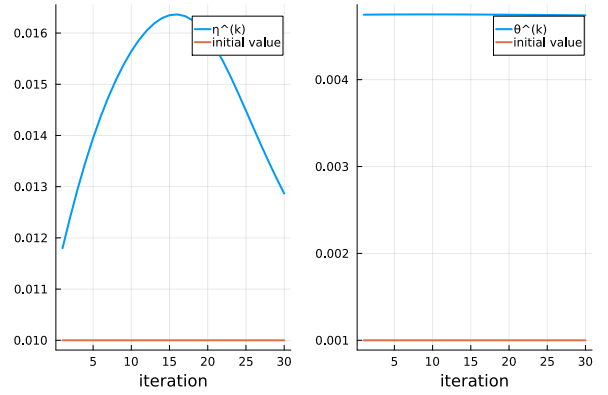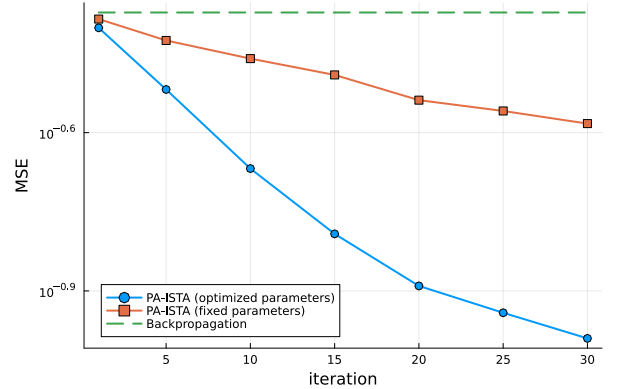

Fig. 3. Tuned parameters by deep unfolding.

Fig. 4. Comparisons of MSE performance of PA-ISTA. SNR is 5 dB.

the true sparse vector and $\hat{\boldsymbol{s}}$ is the PA-ISTA estimate. The expectation is estimated from 100 independent trials. The results demonstrate that PA-ISTA achieves substantially lower MSE values compared to conventional backpropagation methods, whose performance levels are indicated by horizontal lines in the figure. This significant performance gap clearly highlights the advantages of our physics-aware approach over traditional recovery methods. The figure also includes MSE curves for PA-ISTA using fixed initial parameters without DU optimization. These curves exhibit notably slower convergence, as evidenced by their shallower slopes compared to the versions with optimized parameters. This comparison provides compelling evidence for the effectiveness of DU in enhancing reconstruction performance. The optimization of iteration-dependent parameters through DU leads to both faster convergence and better final recovery accuracy.

B. Estimation of NLSE Parameters

Figure 5 illustrates the convergence behavior of the gradient descent process for estimating the NLSE parameters β_2 and γ through the squared error minimization defined in (20). The initial values were set to $\beta_2 = 8$ and $\gamma = 5$, with all other simulation parameters matching those of our previous

experiments. The estimation was performed under an SNR of 5 dB. The trajectories shown in Figure 5 demonstrate gradual convergence of the estimated parameters toward their true values as the iterations progress, exemplifying a successful case of parameter estimation. The smooth convergence behavior suggests that when initialized appropriately, the gradient descent process can effectively navigate the optimization landscape to find accurate parameter estimates.

However, it is important to note that the success of this estimation process is sensitive to initialization. Our experiments revealed that estimation attempts occasionally fail when the initial parameter values are too far from their true values. This sensitivity can be attributed to the non-convex nature of the optimization problem, where the gradient descent process may become trapped in undesirable stationary points. These observations underscore the critical importance of appropriate parameter initialization for achieving reliable estimation results. Accurate calibration of the NLSE parameters is crucial for achieving optimal performance in physics-aware sparse signal recovery, as the reconstruction quality heavily depends on the precision of the underlying physical model.
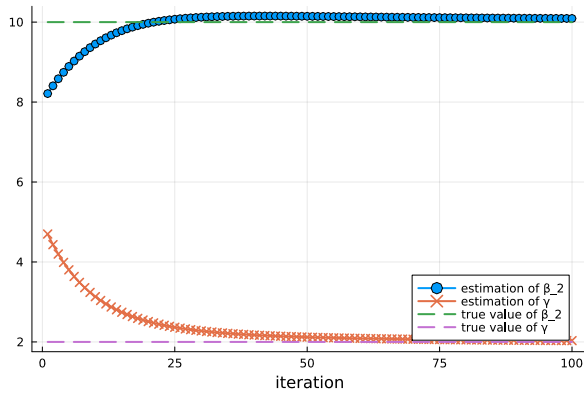

Fig. 5. Parameter estimation via squared error minimization.

VI. CONCLUDING SUMMARY

This paper has presented a physics-aware framework for sparse signal recovery in systems governed by PDEs. By incorporating physical models directly into the recovery process through AD and numerical PDE solvers, our approach demonstrates the potential of *physics-aware signal processing*. The proposed PA-ISTA algorithm, while illustrated through optical fiber applications, establishes a general methodology for integrating physical constraints into sparse recovery problems.

Several promising directions for future research emerge from this work:

1) Non-Gaussian noises: While our current formulation assumes Gaussian noise and employs a quadratic loss function, real-world optical systems often encounter various types of noise with different statistical characteristics, such as shot noise or impulsive noise. Adapting our

physics-aware recovery framework to these scenarios would require reformulating the objective function to incorporate appropriate noise models and developing robust estimation techniques.

2) Extension to other physical systems: The framework developed here could be adapted to other PDE-governed measurement systems, such as heat diffusion processes, acoustic wave propagation, or electromagnetic field reconstruction. For example, in case of electromagnetic field, we can employ Finite-Difference Time-Domain (FDTD) method as a PDE solver. Each application would require careful consideration of appropriate numerical solvers and physical constraints.

3) Computational efficiency: Investigation of more efficient numerical PDE solvers and automatic differentiation mechanisms could further improve the practical applicability of physics-aware recovery methods. This includes exploring adaptive step-size selection in PDE solving processes.

4) Real-world applications: Validation of the proposed framework with experimental data from various physical systems would provide valuable insights into its practical limitations and potential improvements.

The integration of physical models with sparse signal recovery techniques represents a promising direction for signal processing in complex physical systems. As computational capabilities continue to advance, physics-aware approaches may become increasingly practical for a wider range of applications in science and engineering.

REFERENCES

[1] D. L. Donoho, "Compressed sensing," IEEE Trans. Inf. Theory, vol. 52, no. 4, pp. 1289-1306, Apr. 2006.

[2] E. J. Candes and T. Tao, "Near-optimal signal recovery from random projections: Universal encoding strategies?" IEEE Trans. Inf. Theory, vol. 52, no. 12, pp. 5406-5425, Dec. 2006.

[3] Z. Zhang, Y. Xu, J. Yang, X. Li, and D. Zhang, "A survey of sparse representation: Algorithms and applications," IEEE Access, vol. 3, pp. 490-530, May. 2015.

[4] R. Tibshirani, "Regression shrinkage and selection via the lasso," J. Royal Stat. Society, Series B, vol. 58, pp. 267-288, 1996.

[5] B. Efron, T. Hastie, I. Johnstone, and R. Tibshirani, "Least angle regression," Ann. Stat., vol. 32, no. 2, pp. 407-499, Apr. 2004.

[6] A. Chambolle, R. A. DeVore, N. Lee, and B. J. Lucier, "Nonlinear wavelet image processing: Variational problems, compression, and noise removal through wavelet shrinkage," IEEE Trans. Image Process., vol. 7, no. 3, pp. 319-335, Mar. 1998.

[7] I. Daubechies, M. Defrise, and C. De Mol, "An iterative thresholding algorithm for linear inverse problems with a sparsity constraint," Comm. Pure and Appl. Math., vol. 57, no. 11, pp. 1413-1457, Aug. 2004.

[8] M. Raissi, P. Perdikaris and G.E. Karniadakis "Physics-informed neural networks: a deep learning framework for solving forward and inverse problems involving nonlinear partial differential equations," Journal of Computational Physics, Vol. 378, pp.686-707, 2019.

[9] G. P. Agrawal, "Nonlinear Fiber Optics (6th ed.)," Academic Press, 2019.

[10] A. G. Baydin, B. A. Pearlmutter, A. A. Radul, and J. M. Siskind, "Automatic differentiation in machine learning: a survey," *Journal of Machine Learning Research*, vol. 18, pp. 5595–5637, 2018.

[11] S. Bartels, "Numerical Approximation of Partial Differential Equations," Springer International Publishing Switzerland, 2016.

[12] N. Parikh and S. Boyd, "Proximal algorithms," Foundations and Trends in Optimization, vol. 1, no. 3, pp. 123-231, 2014.

[13] E. Ip and J. M. Kahn, "Compensation of dispersion and nonlinear impairments using digital backpropagation," in Journal of Lightwave Technology, vol. 26, no. 20, pp. 3416-3425, 2008.

[14] K. Gregor, and Y. LeCun, "Learning fast approximations of sparse coding," Proc. 27th Int. Conf. Machine Learning, pp. 399-406, 2010.

[15] A. Balatsoukas-Stimming and C. Studer, "Deep unfolding for communications systems: a survey and some new directions," in *Proc. IEEE International Workshop on Signal Processing Systems (SiPS)*, pp. 266–271, 2019.

[16] M. Borgerding, P. Schniter, and S. Rangan, "AMP-inspired deep networks for sparse linear inverse problems, " IEEE Trans, Sig. Process. vol 65, no. 16, pp. 4293-4308 Aug. 2017.

[17] D. Ito, S. Takabe, and T. Wadayama, "Trainable ISTA for sparse signal recovery," IEEE Trans. Sig. Process., vol. 67, no. 12, pp. 3113–3125, Jun. 2019.

[18] D. P. Kingma and J. L. Ba, "Adam: A method for stochastic optimization," arXiv:1412.6980, 2014.

[19] T. Wadayama, K. Igarashi, and T. Takahashi, "Physics-aware decoding for communication channels governed by partial differential equations," submitted to ISIT 2025.